

**Dielectric Constants and Double Layer Formation in a Perovskite Thin Film Revealed by  
Electrochemical Impedance Spectroscopy**

Sauraj Jha, Ross Haroldson, Anvar A. Zakhidov (0000-0003-3983-2229), and Jason D. Slinker  
(0000-0001-7338-586X)

Dr. S. Jha, Prof. A. A. Zakhidov, and Prof. J. D. Slinker

Department of Materials Science and Engineering

The University of Texas at Dallas

800 West Campbell Road, SCI 10, Richardson, Texas 75080-3021, United States

E-mail: slinker@utdallas.edu

Dr. R. Haroldson, Prof. A. A. Zakhidov, and Prof. J. D. Slinker

Department of Physics

The University of Texas at Dallas

800 West Campbell Road, SCI 10, Richardson, Texas 75080-3021, United States

Prof. J. D. Slinker

Department of Chemistry

The University of Texas at Dallas

800 West Campbell Road, SCI 10, Richardson, Texas 75080-3021, United States

Prof. A. A. Zakhidov

NanoTech Institute, The University of Texas at Dallas, 800 West Campbell Road, Richardson,  
Texas 75080-3021, United States.

Prof. A. A. Zakhidov

Samarkand Quantum Center, Samarkand National University, Samarkand, Republic of  
Uzbekistan

## Abstract

Hybrid perovskites have attracted great interest in solar energy conversion and optoelectronic applications. The interconnected ionic and electronic effects complicate assessing the underlying electrical processes while contributing greatly to the efficiency and stability of devices. Fortunately, these coupled processes manifest on distinct timescales that enable frequency-specific electrochemical analysis. However, hybrid perovskites dissolve in most of the common aqueous and organic solvents utilized for electrochemistry. Here, we utilize a hydrofluoroether (HFE) solvent toolkit to perform nondestructive electrochemical impedance spectroscopy of methylammonium lead iodide ( $\text{MAPbI}_3$ ) perovskite thin films. This enables the extraction of dielectric constants and double-layer formation in these perovskite films.

## Keywords

Electrical properties, Ion conductor, Optoelectronic, Thin film, Electronic material

## Introduction

Hybrid perovskites are extensively investigated for their high optoelectronic performance from earth-abundant materials.<sup>1, 2</sup> They are solution-cast to form extensive crystalline networks, producing high mobilities for electron and hole motion.<sup>3, 4</sup> Their electronic and optical properties are tunable through the interchange of the constituent ions and the inclusion of nanocrystalline domains within the films.<sup>5-9</sup> These perovskites are also highly ionically conducting, receiving attention as battery and energy storage applications.<sup>10-12</sup>

This broad landscape for tuning the chemical and structural composition of perovskites and their wide-ranging usage in device applications makes the fundamental study of their inherent

properties crucial for idealized performance and understanding. Solution-based electrochemistry is emerging as a powerful benchtop tool for studying the energy states and electronic properties of various perovskite thin films.<sup>10, 13-20</sup> Still, the organic and inorganic components of hybrid perovskites make it challenging to apply many of the standard electrolytes to perform electrochemical analysis without dissolving the thin film. To perform perovskite electrochemistry with minimal disruption to the crystal structure, we utilize a hydrofluoroether (HFE) electrolyte,<sup>17, 19</sup> an approach that preserves organic and inorganic thin films.

Our approach to separating ionic and electronic information uses impedance spectroscopy, which has been applied successfully to solid-state perovskite devices.<sup>21-22</sup> A small alternating voltage  $V(\omega)$  of a particular angular frequency  $\omega$  is applied,

$$V(\omega) = V_0 \sin(\omega t), \quad (\text{Eq. 1})$$

resulting in a corresponding alternating current  $I(\omega)$

$$I(\omega) = I_0 \sin(\omega t + \varphi), \quad (\text{Eq. 2})$$

with  $\varphi$  representing a phase difference between the voltage and current. Thus, this gives rise to a complex admittance  $Y$  and impedance  $Z$ :

$$Y = \frac{1}{Z} = \frac{I(\omega)}{V(\omega)} = G(\omega) + i\omega C(\omega), \quad (\text{Eq. 3})$$

where  $G(\omega)$  and  $C(\omega)$  are the overall conductance and capacitance of the system. Now, it is possible from this complex impedance to define:

$$Z(\omega) = |Z(\omega)| e^{i\varphi(\omega)}, \quad (\text{Eq. 4})$$

where  $|Z(\omega)|$  is the magnitude or modulus of the impedance and  $\varphi(\omega)$  is the phase angle. From the plots of  $Z(\omega)$  vs.  $\omega$  and  $\varphi(\omega)$  vs.  $\omega$ , the data curves can be fit to an equivalent circuit model. This has the distinct advantage of providing a physical circuit interpretation of constituent processes and the discernment of multiple processes that may be similar in timescales. Alternatively, from

Equation 3, it is possible to perform a complementary analysis with the system-wide  $G(\omega)$  and  $C(\omega)$ :

$$\frac{1}{Z} = \frac{1}{Z_r + iZ_i} = G(\omega) + i\omega C(\omega), \quad (\text{Eq. 5})$$

Where  $Z_r$  is the real part and  $Z_i$  is the imaginary part of  $Z$ . Rationalizing the denominator of Eq. 5, one obtains:

$$\frac{Z_r - iZ_i}{Z_r^2 + Z_i^2} = G(\omega) + i\omega C(\omega). \quad (\text{Eq. 6})$$

Then, connecting the real and imaginary parts, one can obtain the conductance,

$$G(\omega) = \frac{Z_r}{Z_r^2 + Z_i^2}, \quad (\text{Eq. 7})$$

and the capacitance,

$$C(\omega) = \frac{-1}{\omega} \frac{Z_i}{Z_r^2 + Z_i^2}. \quad (\text{Eq. 8})$$

This overall approach provides a complementary complex impedance analysis that offers a direct frequency dependence view of the conductance and capacitance. This is especially important to discern processes that may be smaller in the overall magnitude of impedance (hence hidden by equivalent circuit analysis) but distinct in the timescale of manifestation. Here, we utilize this approach to complex impedance analysis with a HFE electrolyte to analyze the electronic and ionic effects in a methylammonium lead iodide ( $\text{MAPbI}_3$ ) thin film.

## Materials and Methods

*Perovskite Ink Solution Preparation:* A 1:1:1 molar ratio, 1 M perovskite ink of lead iodide, methylammonium acetate, and methylammonium iodide was prepared. Lead (II) iodide (Tokyo Chemical Industry, 99.99%) was dissolved in anhydrous N, N-dimethylformamide (Sigma-Aldrich, 99.8%) by stirring at 550 rpm at 70 °C for 30 mins followed by room-temperature addition

and stirring of methylammonium iodide (Lumtec, 99.5%) and methylammonium acetate (Greatcell Solar Materials), respectively. The solution was stirred for one hour and was filtered using a nylon syringe filter (0.22  $\mu$ m pore size, Aireka Cells) immediately before spin coating.

*Device Fabrication:* Prepatterned ITO/glass substrates (150 nm,  $\sim$ 20  $\Omega$   $\text{sq}^{-1}$ ) were purchased from Thin Film Devices, Inc. These slides were cleaned in a sequence of non-ionic detergent wash, water bath sonication, and UV ozone treatment. The filtered perovskite ink was dispensed at the center of the substrate and was spin-cast with a 5 s ramp time and 60 s spin duration. Films were then placed under vacuum for 90-120 s, followed by 100  $^{\circ}\text{C}$  annealing for 10 mins.

*Electrochemical Testing:* A three-electrode configuration was used for electrochemical measurements with a non-aqueous, no-leak Ag/AgCl reference electrode (eDAQ, Inc.) and a platinum wire as a counter electrode. The electrolyte was prepared by preparing 2.0 M LiPF<sub>6</sub> (battery grade,  $\geq$  99.99% trace metals basis) in diethyl carbonate (DEC, anhydrous,  $\geq$  99%, Sigma-Aldrich). The mixture was then added to a HFE solvent (3M Novec 7500, 3-Ethoxyperfluoro(2-methylhexane)) that had been previously degassed by bubbling argon gas for 60 mins. The final solution was 95% HFE, 5% DEC v/v, 0.1 M LiPF<sub>6</sub>. Electrochemical impedance spectroscopy measurements were performed on a vibration isolation table using a CHI750D Electrochemical Analyzer and a CHI684 multiplexer in a Faraday cage. Films were measured in the dark.

## Results

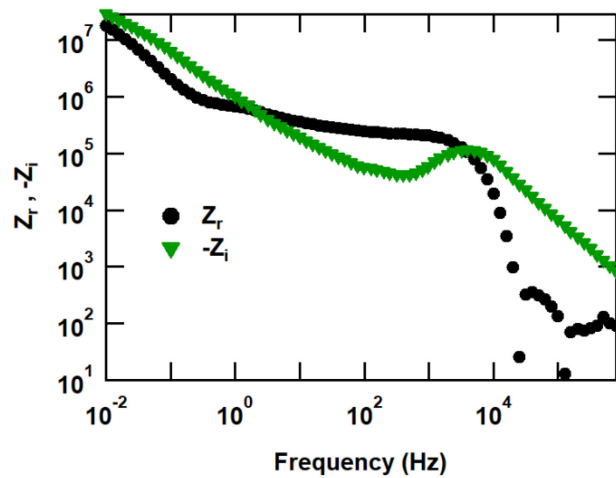


**Figure 1** Bode plot of the real and imaginary components of complex impedance versus frequency for a  $\text{MAPbI}_3$  thin film in a HFE electrolyte.

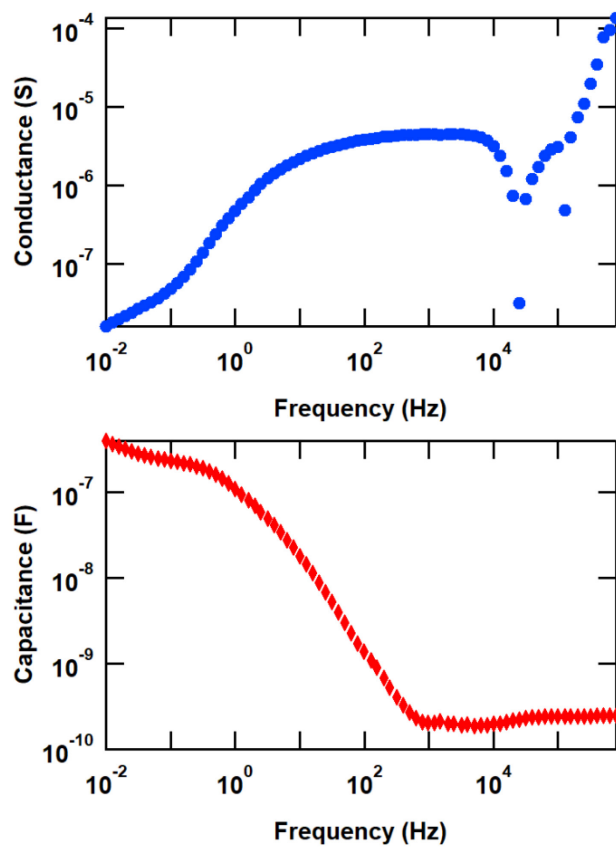


**Figure 2** Bode plot of the overall conductance and capacitance versus frequency for a  $\text{MAPbI}_3$  thin film measured in a HFE electrolyte.

Figure 1 shows the Bode plot of the real and imaginary components of impedance from the electrochemistry of a  $\text{MAPbI}_3$  film. Dynamic behavior is seen in each impedance value throughout this range. Overall,  $Z_r$  and  $Z_i$  are lowered in value as the frequency increases. To gain further insight into the reasons behind this dynamic behavior, the overall conductance and capacitance of the system were calculated according to Equations 7 and 8 and are plotted in Figure 2. Proceeding from right to left on the plot, at high frequency, the conductance drops consistently from 1 MHz to 30 kHz as orientational polarization of the liquid dielectric is anticipated. If a parallel plate capacitor geometry for the film on the circular electrode is assumed, then from the capacitance of 250 pF, a dielectric constant of 5.0 is obtained. This dielectric constant is very similar to the 5.8 value for the Novec 7500 HFE and is likely lowered by the presence of the DEC in the solution. This would imply an intimate solution interaction with the film and correlates well with the initial assumption of orientational polarization at this frequency. The capacitance from 30 kHz to 1 kHz drops to 190 pF. This corresponds to an effective dielectric constant of 3.8 in the parallel plate geometry of the film, which could correlate with the activation of the diethyl carbonate component of the solvent mixture ( $\epsilon = 2.8$  as pure solvent,<sup>23</sup> increases with  $\text{LiPF}_6$  content<sup>24</sup>). The conductance is lowered slightly from 1 kHz to 3 Hz, while capacitance increases significantly. This marks the onset of dielectric polarization in the  $\text{MAPbI}_3$  film, which appears as a peak in the derivative plot of Figure 3. A very subtle change in the capacitance slope is seen near 100 Hz, evident as a peak in the derivative in this region in Figure 3. The capacitance of 2.3 nF at the onset of this feature yields a dielectric constant of 46, very close to the anticipated high-frequency dielectric constant for  $\text{MAPbI}_3$  with ion motion effectively frozen.<sup>25-27</sup> However, the dielectric constant of  $\text{MAPbI}_3$  is frequency-dependent due to the presence of mobile ions. Near 3 Hz, one more peak is apparent

from the derivative plot of Figure 3. The feature at this 3 Hz frequency corresponds to a capacitance of 50 nF and an evident dielectric constant of 990. This is close to the ac dielectric constants obtained for  $\text{MAPbI}_3$  films near this frequency.<sup>25-28</sup> So, this region from 3 Hz to 1 kHz seems to encompass the dielectric behavior of the  $\text{MAPbI}_3$  film, ranging from the smoothly varying ac values to the value near 50. Returning to Figure 2, from 3 Hz to 10 mHz, the conductance drops dramatically as ion motion is activated. The plateau in capacitance near 0.25 Hz corresponds to a capacitance value of 200 nF, the capacitance of double layer formation in the system. These features consistently reproduced over seven independent films.

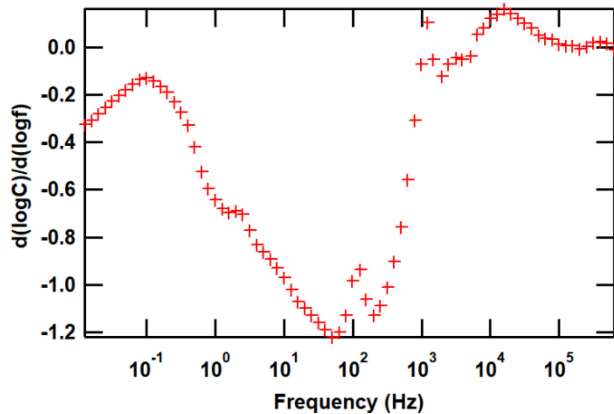


**Figure 3** Numerical midpoint derivative of the logarithm capacitance with respect to the logarithm of the frequency versus frequency for a  $\text{MAPbI}_3$  thin film measured in a HFE electrolyte. This enables the view of dielectric features near 3 Hz, 100 Hz, and 1000 Hz. This particular form of the derivative is chosen to highlight changes in the slope of the capacitance curve presented in Figure 2.

## Discussion

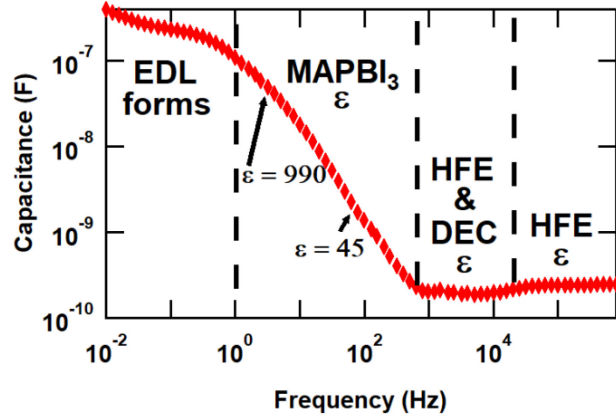


**Figure 4** Summary of the underlying processes contributing to dynamic behavior superimposed on the plot of capacitance versus frequency for a MAPbI<sub>3</sub> thin film measured in a HFE electrolyte.

Overall, we obtain a picture of the contributions to the dynamic impedance, conductance, and capacitive behavior of this system. In Figure 4, we summarize these results on the plot of capacitance versus frequency in Figure 4. Starting at low frequency, electrical double layer (EDL) formation occurs from ion accumulation at the interfaces. Above  $\sim$ 1 Hz, the dielectric behavior of the MAPbI<sub>3</sub> films dominates, proceeding from the ion-assisted AC behavior at lower frequencies to the static limit. At frequencies above  $\sim$ 1 kHz, the solution components dominate, yielding contributions from the DEC and HFE. This approach thus allows us to observe the overall AC dependence of the MAPbI<sub>3</sub> dielectric constant and specific contributions to the system from the electrolyte solution and the electrical double layers.

With the dielectric constant the key factor in the exciton binding energy, which governs recombination losses and thus solar cell efficiency, discerning its value has substantial implications in materials selection and device design. As illustrated, the ionic effects of perovskites complicate the measurement of the dielectric constant, and this approach enables the extraction of the effective

“ion frozen” dielectric constant inherent to the material. This also elucidates the timescales of interest for perovskite study in solution-based electrochemistry as frequencies below 1 kHz.

## Acknowledgments

This article is dedicated to Alex Zakhidov, who co-pioneered the application of orthogonal liquids to the processing of organic materials in electronic devices, particularly for organic photovoltaics, transistors, and LEDs.<sup>29-30</sup> He applied HFE solvents in electrochemical doping and study of perovskites devices.<sup>17,19</sup> He inspired this work, and it is with a great sense of loss that we carry this research forward in his absence. We would also like to thank Muhammad Khalid and Akbar Ali for their help with supporting measurements.

## Conflict of Interests

The authors declare no conflicts of interest.

## Data Availability

The data that support the findings of this study are available from the corresponding author upon reasonable request.

## References

1. J.Y. Kim, J.-W. Lee, H.S. Jung, H. Shin and N.-G. Park: High-Efficiency Perovskite Solar Cells. *Chem. Rev.* **120**, 7867 (2020).
2. N. Yantara, S. Bhaumik, F. Yan, D. Sabba, H.A. Dewi, N. Mathews, P.P. Boix, H.V. Demir and S. Mhaisalkar: Inorganic Halide Perovskites for Efficient Light-Emitting Diodes. *J. Phys. Chem. Lett.* **6**, 4360 (2015).
3. C. Wehrenfennig, G.E. Eperon, M.B. Johnston, H.J. Snaith and L.M. Herz: High Charge Carrier Mobilities and Lifetimes in Organolead Trihalide Perovskites. *Adv. Mater.* **26**, 1584 (2014).
4. C.S. Poncea, T.J. Savenije, M. Abdellah, K.B. Zheng, A. Yartsev, T. Pascher, T. Harlang, P. Chabera, T. Pullerits, A. Stepanov, J.P. Wolf and V. Sundstrom: Organometal Halide

Perovskite Solar Cell Materials Rationalized: Ultrafast Charge Generation, High and Microsecond-Long Balanced Mobilities, and Slow Recombination. *J. Am. Chem. Soc.* **136**, 5189 (2014).

5. J.S. Kim, J.-M. Heo, G.-S. Park, S.-J. Woo, C. Cho, H.J. Yun, D.-H. Kim, J. Park, S.-C. Lee, S.-H. Park, E. Yoon, N.C. Greenham and T.-W. Lee: Ultra-bright, efficient and stable perovskite light-emitting diodes. *Nature* **611**, 688 (2022).
6. L. Protesescu, S. Yakunin, M.I. Bodnarchuk, F. Krieg, R. Caputo, C.H. Hendon, R.X. Yang, A. Walsh and M.V. Kovalenko: Nanocrystals of Cesium Lead Halide Perovskites (CsPbX<sub>3</sub>, X = Cl, Br, and I): Novel Optoelectronic Materials Showing Bright Emission with Wide Color Gamut. *Nano Lett.* **15**, 3692 (2015).
7. D. Ma, K. Lin, Y. Dong, H. Choubisa, A.H. Proppe, D. Wu, Y.-K. Wang, B. Chen, P. Li, J.Z. Fan, F. Yuan, A. Johnston, Y. Liu, Y. Kang, Z.-H. Lu, Z. Wei and E.H. Sargent: Distribution control enables efficient reduced-dimensional perovskite LEDs. *Nature* **599**, 594 (2021).
8. Z. Ren, J. Yu, Z. Qin, J. Wang, J. Sun, C.C.S. Chan, S. Ding, K. Wang, R. Chen, K.S. Wong, X. Lu, W.-J. Yin and W.C.H. Choy: High-Performance Blue Perovskite Light-Emitting Diodes Enabled by Efficient Energy Transfer between Coupled Quasi-2D Perovskite Layers. *Adv. Mater.* **33**, 2005570 (2021).
9. Z. Chen, C. Zhang, X.-F. Jiang, M. Liu, R. Xia, T. Shi, D. Chen, Q. Xue, Y.-J. Zhao, S. Su, H.-L. Yip and Y. Cao: High-Performance Color-Tunable Perovskite Light Emitting Devices through Structural Modulation from Bulk to Layered Film. *Adv. Mater.* **29**, 1603157 (2017).
10. N. Vicente and G. Garcia-Belmonte: Methylammonium Lead Bromide Perovskite Battery Anodes Reversibly Host High Li-Ion Concentrations. *J. Phys. Chem. Lett.* **8**, 1371 (2017).
11. N. Tewari, D. Lam, C.H.A. Li and J.E. Halpert: Recent advancements in batteries and photo-batteries using metal halide perovskites. *APL Mater.* **10** (2022).
12. M.B. Hanif, S. Rauf, M. Motola, Z.U.D. Babar, C.-J. Li and C.-X. Li: Recent progress of perovskite-based electrolyte materials for solid oxide fuel cells and performance optimizing strategies for energy storage applications. *Mater. Res. Bull.* **146**, 111612 (2022).
13. Q.L. Jiang, M.M. Chen, J.Q. Li, M.C. Wang, X.Q. Zeng, T. Besara, J. Lu, Y. Xin, X. Shan, B.C. Pan, C.C. Wang, S.C. Lin, T. Siegrist, Q.F. Xiao and Z.B. Yu: Electrochemical Doping of Halide Perovskites with Ion Intercalation. *ACS Nano* **11**, 1073 (2017).
14. Q. Jiang, X. Zeng, N. Wang, Z. Xiao, Z. Guo and J. Lu: Electrochemical Lithium Doping Induced Property Changes In Halide Perovskite CsPbBr<sub>3</sub> Crystal. *ACS Energy Lett.* **3**, 264 (2018).
15. J.A. Dawson, A.J. Naylor, C. Eames, M. Roberts, W. Zhang, H.J. Snaith, P.G. Bruce and M.S. Islam: Mechanisms of Lithium Intercalation and Conversion Processes in Organic-Inorganic Halide Perovskites. *ACS Energy Lett.* **2**, 1818 (2017).
16. J.T. Mulder, I. du Fosse, M.A. Jazi, L. Manna and A.J. Houtepen: Electrochemical p-Doping of CsPbBr<sub>3</sub> Perovskite Nanocrystals. *ACS Energy Lett.* **6**, 2519 (2021).
17. M. Hasan, S. Venkatesan, D. Lyashenko, J.D. Slinker and A. Zakhidov: Solvent Toolkit for Electrochemical Characterization of Hybrid Perovskite Films. *Anal. Chem.* **89**, 9649 (2017).

18. G.F. Samu, R.A. Scheidt, P.V. Kamat and C. Janáky: Electrochemistry and Spectroelectrochemistry of Lead Halide Perovskite Films: Materials Science Aspects and Boundary Conditions. *Chem. Mat.* **30**, 561 (2018).
19. S. Jha, M. Hasan, N. Khakurel, C.A. Ryan, R. McMullen, A. Mishra, A.V. Malko, A.A. Zakhidov and J.D. Slinker: Electrochemical characterization of halide perovskites: Stability & doping. *Mater. Today Adv.* **13**, 100213 (2022).
20. D. Moia, I. Gelmetti, P. Calado, W. Fisher, M. Stringer, O. Game, Y. Hu, P. Docampo, D. Lidzey, E. Palomares, J. Nelson and P.R.F. Barnes: Ionic-to-electronic current amplification in hybrid perovskite solar cells: ionically gated transistor-interface circuit model explains hysteresis and impedance of mixed conducting devices. *Energy Environ. Sci.* **12**, 1296 (2019).
21. A. Guerrero, J. Bisquert, G. Garcia-Belmonte: Impedance spectroscopy of metal halide perovskite solar cells from the perspective of equivalent circuits. *Chem. Rev.* **121**, 14430 (2021)
22. E. Ghahremanirad, O. Almora, S. Suresh, A. A. Drew, T. H. Chowdhury, A. R. Uhl: Beyond Protocols: Understanding the Electrical Behavior of Perovskite Solar Cells by Impedance Spectroscopy, *Adv. Energy Mater.* **13**, 2204370 (2023).
23. M.A. Rivas and T.P. Iglesias: On permittivity and density of the systems {triglyme+(dimethyl or diethyl carbonate)} and formulation of  $\Delta\epsilon$  in terms of volume or mole fraction. *J. Chem. Thermodyn.* **40**, 1120 (2008).
24. H. Lee, S. Hwang, M. Kim, K. Kwak, J. Lee, Y.-K. Han and H. Lee: Why Does Dimethyl Carbonate Dissociate Li Salt Better Than Other Linear Carbonates? Critical Role of Polar Conformers. *J. Phys. Chem. Lett.* **11**, 10382 (2020).
25. S. Govinda, B.P. Kore, M. Bokdam, P. Mahale, A. Kumar, S. Pal, B. Bhattacharyya, J. Lahnsteiner, G. Kresse, C. Franchini, A. Pandey and D.D. Sarma: Behavior of Methylammonium Dipoles in MAPbX(3) (X = Br and I). *J Phys Chem Lett* **8**, 4113 (2017).
26. M. Sajedi Alvar, P.W.M. Blom and G.-J.A.H. Wetzelaer: Device Model for Methylammonium Lead Iodide Perovskite With Experimentally Validated Ion Dynamics. *Adv. Electron. Mater.* **6**, 1900935 (2020).
27. E.J. Juarez-Perez, R.S. Sanchez, L. Badia, G. Garcia-Belmonte, Y.S. Kang, I. Mora-Sero and J. Bisquert: Photoinduced Giant Dielectric Constant in Lead Halide Perovskite Solar Cells. *J. Phys. Chem. Lett.* **5**, 2390 (2014).
28. M.N.F. Hoque, M. Yang, Z. Li, N. Islam, X. Pan, K. Zhu and Z. Fan: Polarization and Dielectric Study of Methylammonium Lead Iodide Thin Film to Reveal its Nonferroelectric Nature under Solar Cell Operating Conditions. *ACS Energy Lett.* **1**, 142 (2016).
29. A.A. Zakhidov, J.K. Lee, H.H. Fong, J.A. DeFranco, M. Chatzichristidi, P.G. Taylor, C.K. Ober and G.G. Malliaras: Hydrofluoroethers as orthogonal solvents for the chemical processing of organic electronic materials. *Adv. Mater.* **20**, 3481 (2008).
30. A.A. Zakhidov, S. Reineke, B. Lüssem and K. Leo: Hydrofluoroethers as heat-transfer fluids for OLEDs: Operational range, stability, and efficiency improvement. *Org. Electron.* **13**, 356 (2012).

## **Author Contributions**

Conceptualization, Sauraj Jha, Ross Haroldson, and Jason Slinker; Data curation, Sauraj Jha and Ross Haroldson; Formal analysis, Sauraj Jha, Ross Haroldson, Anvar Zakhidov, and Jason Slinker; Funding acquisition, Anvar Zakhidov and Jason Slinker; Investigation, Sauraj Jha, Ross Haroldson, Anvar Zakhidov, and Jason Slinker; Project administration, Jason Slinker; Supervision, Anvar Zakhidov and Jason Slinker; Validation, Sauraj Jha; Writing – original draft, Jason Slinker; Writing – review & editing, Sauraj Jha, Ross Haroldson, Anvar Zakhidov, and Jason Slinker.

## **Funding**

J.D.S. acknowledges support from the National Science Foundation Electrical, Communications and Cyber Systems (ECCS 1906505). A.Z. acknowledges support from the Welch Foundation (AT-1617) and the Russian Science Foundation (19-73-30023).

## **Supplementary Information**

### **Dielectric Constants and Double Layer Formation in a Perovskite Thin Film Revealed by Electrochemical Impedance Spectroscopy**

Sauraj Jha, Ross Haroldson, Anvar A. Zakhidov (0000-0003-3983-2229), and Jason D. Slinker (0000-0001-7338-586X)

Dr. S. Jha, Prof. A. A. Zakhidov, and Prof. J. D. Slinker

Department of Materials Science and Engineering

The University of Texas at Dallas

800 West Campbell Road, SCI 10, Richardson, Texas 75080-3021, United States

E-mail: [slinker@utdallas.edu](mailto:slinker@utdallas.edu)

Dr. R. Haroldson, Prof. A. A. Zakhidov, and Prof. J. D. Slinker

Department of Physics

The University of Texas at Dallas

800 West Campbell Road, SCI 10, Richardson, Texas 75080-3021, United States

Prof. J. D. Slinker

Department of Chemistry

The University of Texas at Dallas

800 West Campbell Road, SCI 10, Richardson, Texas 75080-3021, United States

Prof. A. A. Zakhidov

NanoTech Institute, The University of Texas at Dallas, 800 West Campbell Road, Richardson, Texas 75080-3021, United States.

Prof. A. A. Zakhidov

Samarkand Quantum Center, Samarkand National University, Samarkand, Republic of Uzbekistan

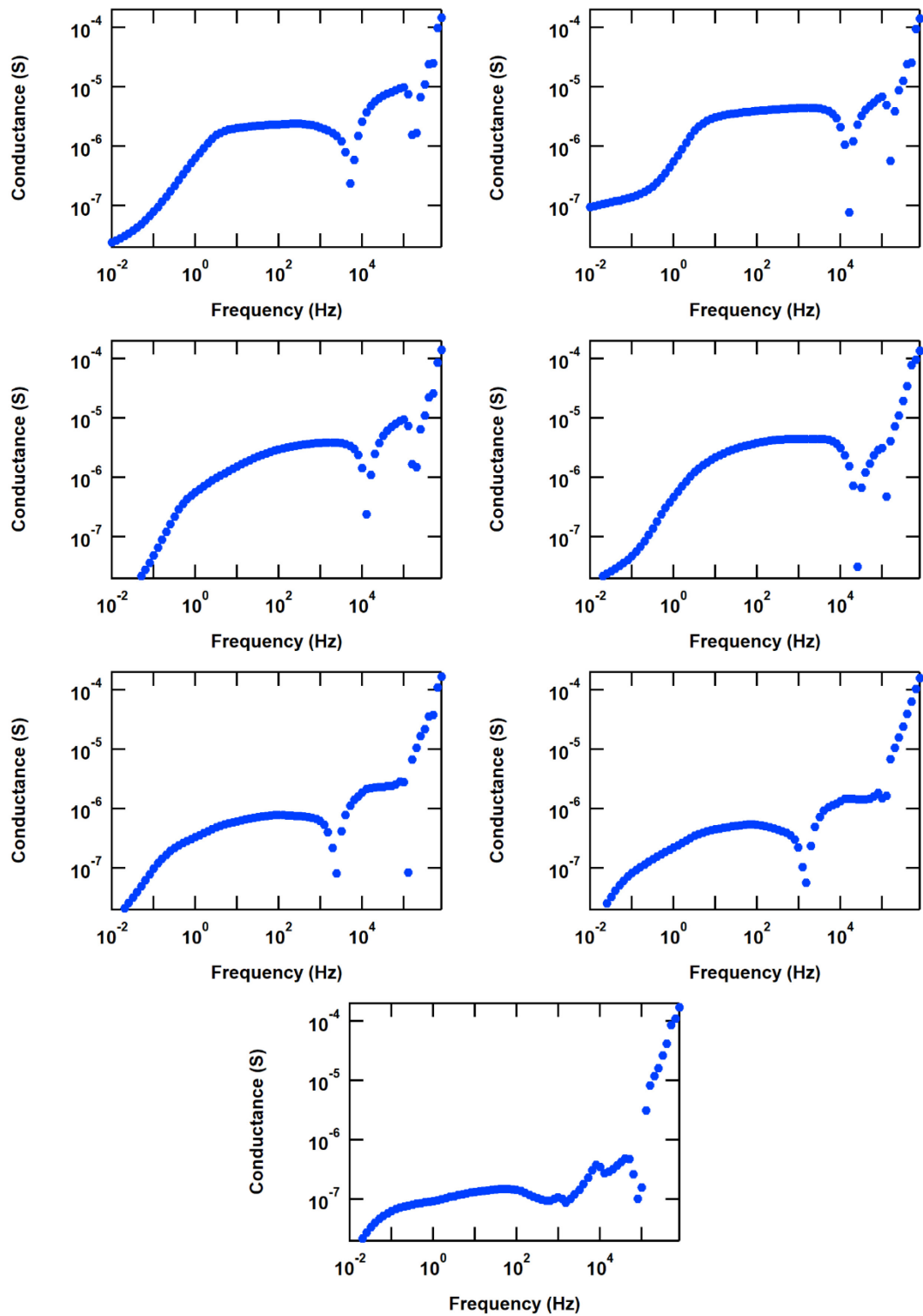


**Figure S1** Conductance versus frequency for the seven  $\text{MAPbI}_3$ /ITO in HFE electrolyte samples of this study.

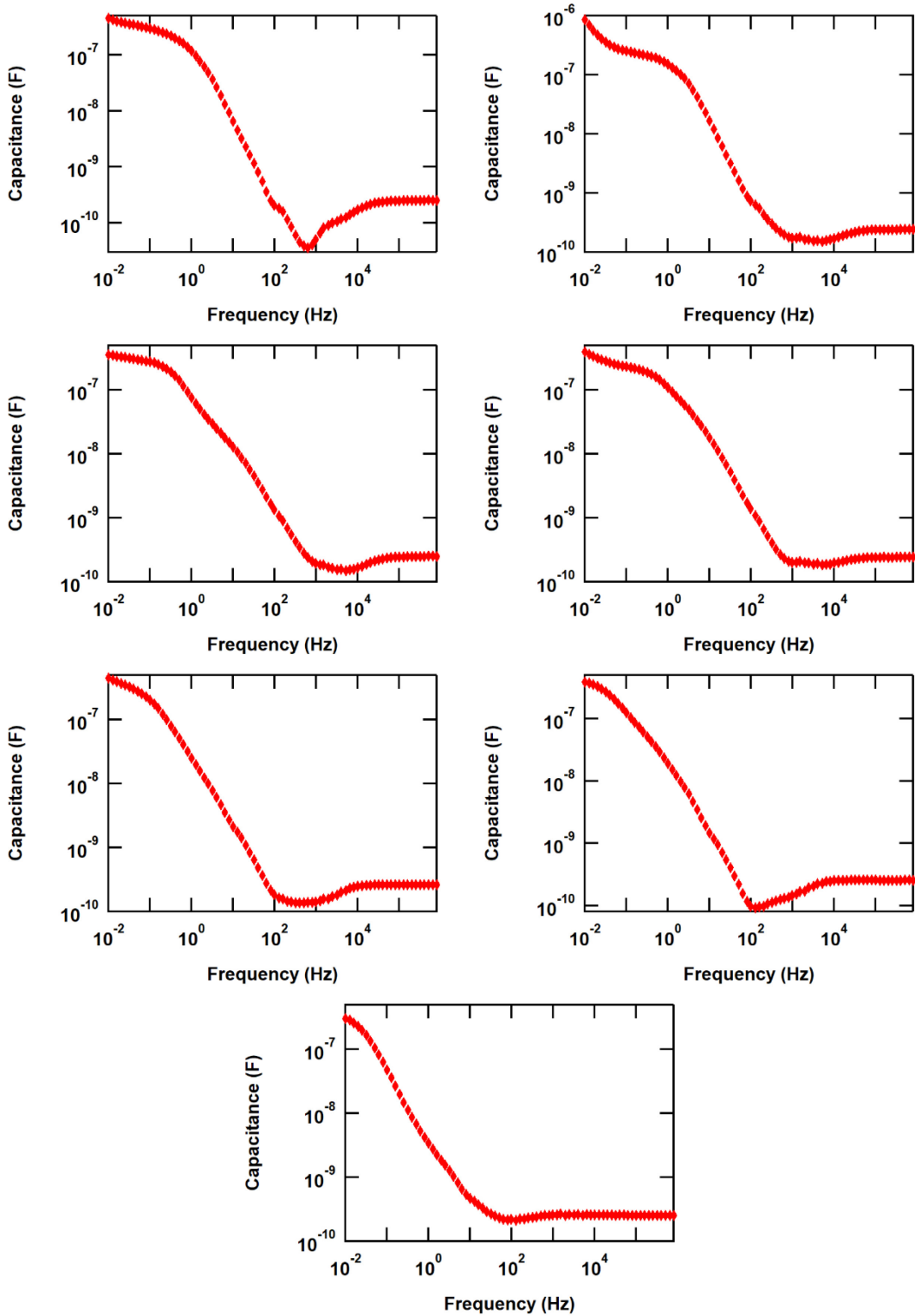


**Figure S2** Capacitance versus frequency for the seven  $\text{MAPbI}_3/\text{ITO}$  in HFE electrolyte samples of this study.